BABAR-CONF-03/009
SLAC-PUB-9692
March 2003

Observation of B Meson Decays to $\eta\pi$ and ηK

Abstract

We present preliminary measurements of the B meson decays $B^+ \to \eta\pi^+$, $B^+ \to \eta K^+$, and $B^0 \to \eta K^0$. The data were recorded with the BABAR detector at PEP II and correspond to 88.9×10^6 $B\overline{B}$ pairs produced in e^+e^- annihilation through the $\Upsilon(4S)$ resonance. We find the branching fractions $\mathcal{B}(B^+ \to \eta\pi^+) = (4.2^{+1.0}_{-0.9} \pm 0.3) \times 10^{-6}$ and $\mathcal{B}(B^+ \to \eta K^+) = (2.8^{+0.8}_{-0.7} \pm 0.2) \times 10^{-6}$. We set a 90% CL upper limit of $\mathcal{B}(B^0 \to \eta K^0) < 4.6 \times 10^{-6}$. The time-integrated charge asymmetries are $\mathcal{A}_{ch}(B^+ \to \eta\pi^+) = -0.51^{+0.20}_{-0.18} \pm 0.01$ and $\mathcal{A}_{ch}(B^+ \to \eta K^+) = -0.32^{+0.22}_{-0.18} \pm 0.01$.

Presented at the XXXVIIIth Rencontres de Moriond on
QCD and High Energy Hadronic Interactions,
3/22—3/29/2003, Les Arcs, Savoie, France

Stanford Linear Accelerator Center, Stanford University, Stanford, CA 94309

Work supported in part by Department of Energy contract DE-AC03-76SF00515.

The *BABAR* Collaboration,

B. Aubert, R. Barate, D. Boutigny, J.-M. Gaillard, A. Hicheur, Y. Karyotakis, J. P. Lees, P. Robbe, V. Tisserand, A. Zghiche

Laboratoire de Physique des Particules, F-74941 Annecy-le-Vieux, France

A. Palano, A. Pompili

Università di Bari, Dipartimento di Fisica and INFN, I-70126 Bari, Italy

J. C. Chen, N. D. Qi, G. Rong, P. Wang, Y. S. Zhu

Institute of High Energy Physics, Beijing 100039, China

G. Eigen, I. Ofte, B. Stugu

University of Bergen, Inst. of Physics, N-5007 Bergen, Norway

G. S. Abrams, A. W. Borgland, A. B. Breon, D. N. Brown, J. Button-Shafer, R. N. Cahn, E. Charles, C. T. Day, M. S. Gill, A. V. Gritsan, Y. Groysman, R. G. Jacobsen, R. W. Kadel, J. Kadyk, L. T. Kerth, Yu. G. Kolomensky, J. F. Kral, G. Kukartsev, C. LeClerc, M. E. Levi, G. Lynch, L. M. Mir, P. J. Oddone, T. J. Orimoto, M. Pripstein, N. A. Roe, A. Romosan, M. T. Ronan, V. G. Shelkov, A. V. Telnov, W. A. Wenzel

Lawrence Berkeley National Laboratory and University of California, Berkeley, CA 94720, USA

T. J. Harrison, C. M. Hawkes, D. J. Knowles, R. C. Penny, A. T. Watson, N. K. Watson

University of Birmingham, Birmingham, B15 2TT, United Kingdom

T. Deppermann, K. Goetzen, H. Koch, B. Lewandowski, M. Pelizaeus, K. Peters, H. Schmuecker, M. Steinke

Ruhr Universität Bochum, Institut für Experimentalphysik 1, D-44780 Bochum, Germany

N. R. Barlow, W. Bhimji, J. T. Boyd, N. Chevalier, W. N. Cottingham, C. Mackay, F. F. Wilson

University of Bristol, Bristol BS8 1TL, United Kingdom

C. Hearty, T. S. Mattison, J. A. McKenna, D. Thiessen

University of British Columbia, Vancouver, BC, Canada V6T 1Z1

P. Kyberd, A. K. McKemey

Brunel University, Uxbridge, Middlesex UB8 3PH, United Kingdom

V. E. Blinov, A. D. Bukin, V. B. Golubev, V. N. Ivanchenko, E. A. Kravchenko, A. P. Onuchin, S. I. Serednyakov, Yu. I. Skovpen, E. P. Solodov, A. N. Yushkov

Budker Institute of Nuclear Physics, Novosibirsk 630090, Russia

D. Best, M. Chao, D. Kirkby, A. J. Lankford, M. Mandelkern, S. McMahon, R. K. Mommsen, W. Roethel, D. P. Stoker

University of California at Irvine, Irvine, CA 92697, USA

C. Buchanan

University of California at Los Angeles, Los Angeles, CA 90024, USA

H. K. Hadavand, E. J. Hill, D. B. MacFarlane, H. P. Paar, Sh. Rahatlou, U. Schwanke, V. Sharma

University of California at San Diego, La Jolla, CA 92093, USA

J. W. Berryhill, C. Campagnari, B. Dahmes, N. Kuznetsova, S. L. Levy, O. Long, A. Lu, M. A. Mazur, J. D. Richman, W. Verkerke

University of California at Santa Barbara, Santa Barbara, CA 93106, USA

J. Beringer, A. M. Eisner, C. A. Heusch, W. S. Lockman, T. Schalk, R. E. Schmitz, B. A. Schumm, A. Seiden, M. Turri, W. Walkowiak, D. C. Williams, M. G. Wilson

University of California at Santa Cruz, Institute for Particle Physics, Santa Cruz, CA 95064, USA

J. Albert, E. Chen, M. P. Dorsten, G. P. Dubois-Felsmann, A. Dvoretskii, D. G. Hitlin, I. Narsky, F. C. Porter, A. Ryd, A. Samuel, S. Yang

California Institute of Technology, Pasadena, CA 91125, USA

S. Jayatilleke, G. Mancinelli, B. T. Meadows, M. D. Sokoloff

University of Cincinnati, Cincinnati, OH 45221, USA

T. Barillari, F. Blanc, P. Bloom, P. J. Clark, W. T. Ford, C. L. Lee, U. Nauenberg, A. Olivas, P. Rankin, J. Roy, J. G. Smith, W. C. van Hoek, L. Zhang

University of Colorado, Boulder, CO 80309, USA

J. L. Harton, T. Hu, A. Soffer, W. H. Toki, R. J. Wilson, J. Zhang

Colorado State University, Fort Collins, CO 80523, USA

D. Altenburg, T. Brandt, J. Brose, T. Colberg, M. Dickopp, R. S. Dubitzky, A. Hauke, H. M. Lacker, E. Maly, R. Müller-Pfefferkorn, R. Nogowski, S. Otto, K. R. Schubert, R. Schwierz, B. Spaan, L. Wilden

Technische Universität Dresden, Institut für Kern- und Teilchenphysik, D-01062 Dresden, Germany

D. Bernard, G. R. Bonneaud, F. Brochard, J. Cohen-Tanugi, Ch. Thiebaux, G. Vasileiadis, M. Verderi

Ecole Polytechnique, LLR, F-91128 Palaiseau, France

A. Khan, D. Lavin, F. Muheim, S. Playfer, J. E. Swain, J. Tinslay

University of Edinburgh, Edinburgh EH9 3JZ, United Kingdom

C. Bozzi, L. Piemontese, A. Sarti

Università di Ferrara, Dipartimento di Fisica and INFN, I-44100 Ferrara, Italy

E. Treadwell

Florida A&M University, Tallahassee, FL 32307, USA

F. Anulli,[1] R. Baldini-Ferroli, A. Calcaterra, R. de Sangro, D. Falciai, G. Finocchiaro, P. Patteri, I. M. Peruzzi,[1] M. Piccolo, A. Zallo

Laboratori Nazionali di Frascati dell'INFN, I-00044 Frascati, Italy

A. Buzzo, R. Contri, G. Crosetti, M. Lo Vetere, M. Macri, M. R. Monge, S. Passaggio, F. C. Pastore, C. Patrignani, E. Robutti, A. Santroni, S. Tosi

Università di Genova, Dipartimento di Fisica and INFN, I-16146 Genova, Italy

S. Bailey, M. Morii

Harvard University, Cambridge, MA 02138, USA

[1]Also with Università di Perugia, Perugia, Italy

G. J. Grenier, S.-J. Lee, U. Mallik
University of Iowa, Iowa City, IA 52242, USA

J. Cochran, H. B. Crawley, J. Lamsa, W. T. Meyer, S. Prell, E. I. Rosenberg, J. Yi
Iowa State University, Ames, IA 50011-3160, USA

M. Davier, G. Grosdidier, A. Höcker, S. Laplace, F. Le Diberder, V. Lepeltier, A. M. Lutz, T. C. Petersen, S. Plaszczynski, M. H. Schune, L. Tantot, G. Wormser
Laboratoire de l'Accélérateur Linéaire, F-91898 Orsay, France

R. M. Bionta, V. Brigljević , C. H. Cheng, D. J. Lange, D. M. Wright
Lawrence Livermore National Laboratory, Livermore, CA 94550, USA

A. J. Bevan, J. R. Fry, E. Gabathuler, R. Gamet, M. Kay, D. J. Payne, R. J. Sloane, C. Touramanis
University of Liverpool, Liverpool L69 3BX, United Kingdom

M. L. Aspinwall, D. A. Bowerman, P. D. Dauncey, U. Egede, I. Eschrich, G. W. Morton, J. A. Nash, P. Sanders, G. P. Taylor
University of London, Imperial College, London, SW7 2BW, United Kingdom

J. J. Back, G. Bellodi, P. F. Harrison, H. W. Shorthouse, P. Strother, P. B. Vidal
Queen Mary, University of London, E1 4NS, United Kingdom

G. Cowan, H. U. Flaecher, S. George, M. G. Green, A. Kurup, C. E. Marker, T. R. McMahon, S. Ricciardi, F. Salvatore, G. Vaitsas, M. A. Winter
University of London, Royal Holloway and Bedford New College, Egham, Surrey TW20 0EX, United Kingdom

D. Brown, C. L. Davis
University of Louisville, Louisville, KY 40292, USA

J. Allison, R. J. Barlow, A. C. Forti, P. A. Hart, F. Jackson, G. D. Lafferty, A. J. Lyon, J. H. Weatherall, J. C. Williams
University of Manchester, Manchester M13 9PL, United Kingdom

A. Farbin, A. Jawahery, D. Kovalskyi, C. K. Lae, V. Lillard, D. A. Roberts
University of Maryland, College Park, MD 20742, USA

G. Blaylock, C. Dallapiccola, K. T. Flood, S. S. Hertzbach, R. Kofler, V. B. Koptchev, T. B. Moore, H. Staengle, S. Willocq
University of Massachusetts, Amherst, MA 01003, USA

R. Cowan, G. Sciolla, F. Taylor, R. K. Yamamoto
Massachusetts Institute of Technology, Laboratory for Nuclear Science, Cambridge, MA 02139, USA

D. J. J. Mangeol, M. Milek, P. M. Patel
McGill University, Montréal, QC, Canada H3A 2T8

A. Lazzaro, F. Palombo
Università di Milano, Dipartimento di Fisica and INFN, I-20133 Milano, Italy

J. M. Bauer, L. Cremaldi, V. Eschenburg, R. Godang, R. Kroeger, J. Reidy, D. A. Sanders, D. J. Summers, H. W. Zhao

University of Mississippi, University, MS 38677, USA

C. Hast, P. Taras

Université de Montréal, Laboratoire René J. A. Lévesque, Montréal, QC, Canada H3C 3J7

H. Nicholson

Mount Holyoke College, South Hadley, MA 01075, USA

C. Cartaro, N. Cavallo, G. De Nardo, F. Fabozzi,[2] C. Gatto, L. Lista, P. Paolucci, D. Piccolo, C. Sciacca

Università di Napoli Federico II, Dipartimento di Scienze Fisiche and INFN, I-80126, Napoli, Italy

M. A. Baak, G. Raven

NIKHEF, National Institute for Nuclear Physics and High Energy Physics, 1009 DB Amsterdam, The Netherlands

J. M. LoSecco

University of Notre Dame, Notre Dame, IN 46556, USA

T. A. Gabriel

Oak Ridge National Laboratory, Oak Ridge, TN 37831, USA

B. Brau, T. Pulliam

Ohio State University, Columbus, OH 43210, USA

J. Brau, R. Frey, M. Iwasaki, C. T. Potter, N. B. Sinev, D. Strom, E. Torrence

University of Oregon, Eugene, OR 97403, USA

F. Colecchia, A. Dorigo, F. Galeazzi, M. Margoni, M. Morandin, M. Posocco, M. Rotondo, F. Simonetto, R. Stroili, G. Tiozzo, C. Voci

Università di Padova, Dipartimento di Fisica and INFN, I-35131 Padova, Italy

M. Benayoun, H. Briand, J. Chauveau, P. David, Ch. de la Vaissière, L. Del Buono, O. Hamon, Ph. Leruste, J. Ocariz, M. Pivk, L. Roos, J. Stark, S. T'Jampens

Universités Paris VI et VII, Lab de Physique Nucléaire H. E., F-75252 Paris, France

P. F. Manfredi, V. Re

Università di Pavia, Dipartimento di Elettronica and INFN, I-27100 Pavia, Italy

L. Gladney, Q. H. Guo, J. Panetta

University of Pennsylvania, Philadelphia, PA 19104, USA

C. Angelini, G. Batignani, S. Bettarini, M. Bondioli, F. Bucci, G. Calderini, M. Carpinelli, F. Forti, M. A. Giorgi, A. Lusiani, G. Marchiori, F. Martinez-Vidal,[3] M. Morganti, N. Neri, E. Paoloni, M. Rama, G. Rizzo, F. Sandrelli, J. Walsh

Università di Pisa, Dipartimento di Fisica, Scuola Normale Superiore and INFN, I-56127 Pisa, Italy

[2]Also with Università della Basilicata, Potenza, Italy

[3]Also with IFIC, Instituto de Física Corpuscular, CSIC-Universidad de Valencia, Valencia, Spain

M. Haire, D. Judd, K. Paick, D. E. Wagoner
Prairie View A&M University, Prairie View, TX 77446, USA

N. Danielson, P. Elmer, C. Lu, V. Miftakov, J. Olsen, A. J. S. Smith, E. W. Varnes
Princeton University, Princeton, NJ 08544, USA

F. Bellini, G. Cavoto,[4] D. del Re, R. Faccini,[5] F. Ferrarotto, F. Ferroni, M. Gaspero, E. Leonardi, M. A. Mazzoni, S. Morganti, M. Pierini, G. Piredda, F. Safai Tehrani, M. Serra, C. Voena
Università di Roma La Sapienza, Dipartimento di Fisica and INFN, I-00185 Roma, Italy

S. Christ, G. Wagner, R. Waldi
Universität Rostock, D-18051 Rostock, Germany

T. Adye, N. De Groot, B. Franek, N. I. Geddes, G. P. Gopal, E. O. Olaiya, S. M. Xella
Rutherford Appleton Laboratory, Chilton, Didcot, Oxon, OX11 0QX, United Kingdom

R. Aleksan, S. Emery, A. Gaidot, S. F. Ganzhur, P.-F. Giraud, G. Hamel de Monchenault, W. Kozanecki, M. Langer, G. W. London, B. Mayer, G. Schott, G. Vasseur, Ch. Yeche, M. Zito
DAPNIA, Commissariat à l'Energie Atomique/Saclay, F-91191 Gif-sur-Yvette, France

M. V. Purohit, A. W. Weidemann, F. X. Yumiceva
University of South Carolina, Columbia, SC 29208, USA

D. Aston, R. Bartoldus, N. Berger, A. M. Boyarski, O. L. Buchmueller, M. R. Convery, D. P. Coupal, D. Dong, J. Dorfan, D. Dujmic, W. Dunwoodie, R. C. Field, T. Glanzman, S. J. Gowdy, E. Grauges-Pous, T. Hadig, V. Halyo, T. Hryn'ova, W. R. Innes, C. P. Jessop, M. H. Kelsey, P. Kim, M. L. Kocian, U. Langenegger, D. W. G. S. Leith, S. Luitz, V. Luth, H. L. Lynch, H. Marsiske, S. Menke, R. Messner, D. R. Muller, C. P. O'Grady, V. E. Ozcan, A. Perazzo, M. Perl, S. Petrak, B. N. Ratcliff, S. H. Robertson, A. Roodman, A. A. Salnikov, R. H. Schindler, J. Schwiening, G. Simi, A. Snyder, A. Soha, J. Stelzer, D. Su, M. K. Sullivan, H. A. Tanaka, J. Va'vra, S. R. Wagner, M. Weaver, A. J. R. Weinstein, W. J. Wisniewski, D. H. Wright, C. C. Young
Stanford Linear Accelerator Center, Stanford, CA 94309, USA

P. R. Burchat, T. I. Meyer, C. Roat
Stanford University, Stanford, CA 94305-4060, USA

S. Ahmed, J. A. Ernst
State Univ. of New York, Albany, NY 12222, USA

W. Bugg, M. Krishnamurthy, S. M. Spanier
University of Tennessee, Knoxville, TN 37996, USA

R. Eckmann, H. Kim, J. L. Ritchie, R. F. Schwitters
University of Texas at Austin, Austin, TX 78712, USA

J. M. Izen, I. Kitayama, X. C. Lou, S. Ye
University of Texas at Dallas, Richardson, TX 75083, USA

[4]Also with Princeton University, Princeton, NJ 08544, USA
[5]Also with University of California at San Diego, La Jolla, CA 92093, USA

F. Bianchi, M. Bona, F. Gallo, D. Gamba

Università di Torino, Dipartimento di Fisica Sperimentale and INFN, I-10125 Torino, Italy

C. Borean, L. Bosisio, G. Della Ricca, S. Dittongo, S. Grancagnolo, L. Lanceri, P. Poropat,[6] L. Vitale, G. Vuagnin

Università di Trieste, Dipartimento di Fisica and INFN, I-34127 Trieste, Italy

R. S. Panvini

Vanderbilt University, Nashville, TN 37235, USA

Sw. Banerjee, C. M. Brown, D. Fortin, P. D. Jackson, R. Kowalewski, J. M. Roney

University of Victoria, Victoria, BC, Canada V8W 3P6

H. R. Band, S. Dasu, M. Datta, A. M. Eichenbaum, H. Hu, J. R. Johnson, R. Liu, F. Di Lodovico, A. K. Mohapatra, Y. Pan, R. Prepost, S. J. Sekula, J. H. von Wimmersperg-Toeller, J. Wu, S. L. Wu, Z. Yu

University of Wisconsin, Madison, WI 53706, USA

H. Neal

Yale University, New Haven, CT 06511, USA

[6]Deceased

1 Introduction

We report the results of searches for B decays to the charmless final states[1] $\eta\pi^+$, ηK^+, and ηK^0. We reconstruct the η mesons in both of the dominant final states $\eta \to \gamma\gamma$ ($\eta_{\gamma\gamma}$) and $\eta \to \pi^+\pi^-\pi^0$ ($\eta_{3\pi}$). The K^0 is reconstructed as $K^0_S \to \pi^+\pi^-$. For the charged modes we also measure the direct *CP*-violating time-integrated charge asymmetry, $\mathcal{A}_{ch} = (\Gamma^- - \Gamma^+)/(\Gamma^- + \Gamma^+)$, where $\Gamma^\pm \equiv \Gamma(B^\pm \to \eta h^\pm)$.

The interest in these decays was sparked by the first reports of the observation of the decay $B \to \eta' K$ [1] in 1997. It had been pointed out by Lipkin six years earlier [2] that interference between two penguin diagrams and the known η/η' mixing angle conspire to greatly enhance $B \to \eta' K$ and suppress $B \to \eta K$. Due to a parity flip for the vector K^*, the situation is reversed for the $B \to \eta' K^*$ and $B \to \eta K^*$ decays. Though the general features of this picture have already been borne out by previous measurements and limits, the details and possible contributions of singlet diagrams will only be tested with the measurement of the branching fraction of all four $(\eta, \eta')(K, K^*)$ decays.

It was pointed out more than 20 years ago (before the discovery of the B meson) by Bander, Soni and Silverman [3] that penguin loop diagrams allow substantial ($\gtrsim 20\%$) charge asymmetries in some B decays, and an example they gave was $B \to \eta K$. The necessary ingredients are to have two interfering diagrams with different weak and strong phases. More recently, it was pointed out that such charge asymmetries can be enhanced in $B \to \eta' \pi$ and $B \to \eta\pi$ where the decay rate is small but penguin-tree or penguin-penguin interference is possible [4, 5]. A series of quantitative predictions have been made in the past decade with various factorization approaches [6, 7, 8, 9]. There is general agreement that modes such as $B \to \eta K$, $B \to \eta\pi$, and $B \to \eta'\pi$ are expected to have charge asymmetries of 20% or larger. Most, but not all, of the quantitative calculations predict negative values for all three decays. A recent paper [10] shows that branching fraction and charge asymmetry measurements for $B \to \eta'\pi$ and $B \to \eta\pi$ allow for the determination of the strong phase difference between tree and penguin amplitudes and the CKM angle alpha.

The current knowledge of these decays comes from published measurements from CLEO [11] and conference results from *BABAR* [12] and Belle [13]. Table 1 summarizes these previous results. We present here analyses incorporating new data.

2 Detector and Data

The results presented in this paper are based on data collected in 1999–2002 with the *BABAR* detector [14] at the PEP-II asymmetric e^+e^- collider [15] located at the Stanford Linear Accelerator Center. An integrated luminosity of 81.9 fb^{-1}, corresponding to 88.9 million $B\overline{B}$ pairs, was recorded at the $\Upsilon(4S)$ resonance ("on-resonance", center-of-mass energy $\sqrt{s} = 10.58$ GeV). An additional 9.6 fb^{-1} were taken about 40 MeV below this energy ("off-resonance") for the study of continuum backgrounds in which a light or charm quark pair is produced instead of an $\Upsilon(4S)$.

The asymmetric beam configuration in the laboratory frame provides a boost of $\beta\gamma = 0.56$ to the $\Upsilon(4S)$. Charged particles are detected and their momenta measured by the combination of a silicon vertex tracker (SVT), consisting of five layers of double-sided detectors, and a 40-layer central drift chamber, both operating in the 1.5-T magnetic field of a solenoid. Photons and electrons are detected by a CsI(Tl) electromagnetic calorimeter (EMC).

Charged-particle identification (PID) is provided by the average energy loss (dE/dx) in the tracking devices and by an internally reflecting ring-imaging Cherenkov detector (DIRC) covering

[1] Except as noted explicitly, we use a particle name to denote either member of a charge conjugate pair.

Table 1: Summary of branching fraction results for B decays to η mesons from CLEO [11], previous *BABAR* [12] measurements, Belle [13], and the present analysis. The results for all fits are given as well as a 90% CL upper limit if the measured yield is not judged to be significant. The overall yields and efficiencies (ϵ) are given as the sum of yields and efficiencies from the two η decay channels.

Expt.	# $B\overline{B}$ ($\times 10^6$)	Fit $\mathcal{B}(\times 10^{-6})$	UL $\mathcal{B}(\times 10^{-6})$	Signif. (σ)	Signal yield	ϵ (%)
$B^+ \to \eta\pi^+$						
CLEO	10	$1.2^{+2.8}_{-1.2}$	5.7	0.6	5.7	25.0
BABAR	23	$2.2^{+1.8}_{-1.6} \pm 0.1$	5.2	1.5	8.0	15.8
Belle	32	$5.4^{+2.0}_{-1.7} \pm 0.6$	—	4.3	15.4	9.5
This result	89	$4.2^{+1.0}_{-0.9} \pm 0.3$	—	7.0	67.6	16.5
$B^+ \to \eta K^+$						
CLEO	10	$2.2^{+2.8}_{-2.2}$	6.9	0.8	5.9	24.1
BABAR	23	$3.8^{+1.8}_{-1.5} \pm 0.2$	6.4	3.7	12.9	15.6
Belle	32	$5.3^{+1.8}_{-1.5} \pm 0.6$	—	4.9	16.9	10.6
This result	89	$2.8^{+0.8}_{-0.7} \pm 0.2$	—	6.2	48.7	17.2
$B^0 \to \eta K^0$						
CLEO	10	$0.0^{+3.2}_{-0.0}$	9.3	0.0	0.0	7.0
BABAR	23	$6.0^{+3.8}_{-2.9} \pm 0.4$	12.2	3.2	5.7	4.2
This result	89	$2.6^{+0.9}_{-0.8} \pm 0.2$	4.6	3.3	11.2	5.1

the central region.

3 Event Selection

Monte Carlo (MC) simulations [16] of the signal decay modes and of continuum and $B\overline{B}$ backgrounds are used to establish the event selection criteria. The selection is designed to achieve high efficiency and retain sidebands sufficient to characterize the background for subsequent fitting. Photons must have energy exceeding a threshold dependent on the combinatoric background of the specific mode: $E_\gamma > 30$ MeV for the two photons used to reconstruct the π^0 in $\eta \to \pi^+\pi^-\pi^0$ candidates, and $E_\gamma > 100$ MeV for $\eta \to \gamma\gamma$. Additionally, we require that the cosine of the center of mass decay angle for $\eta_{\gamma\gamma}$ daughters, relative to the flight direction of the η, have an absolute value of less than 0.95 (0.97) for neutral (charged) decays involving the $\eta_{\gamma\gamma}$.

We select $\eta_{\gamma\gamma}$, $\eta_{3\pi}$, and π^0 candidates with the following requirements on the invariant mass in MeV/c^2 of their final states: $490 < m_\eta < 600$ for $\eta_{\gamma\gamma}$, $520 < m_\eta < 570$ for $\eta_{3\pi}$, and $120 < m_{\pi^0} < 150$. For $K^0_S \to \pi^+\pi^-$ candidates we require $488 < m_{K_S} < 508$. Typical resolutions are about 16 MeV/c^2 for $\eta_{\gamma\gamma}$, 4.5 MeV/c^2 for $\eta_{3\pi}$, 2.8 MeV/c^2 for K^0_S, and 7 MeV/c^2 for π^0. For K^0_S candidates we require that the three-dimensional flight distance from the event primary vertex be > 2 mm,

and the two-dimensional angle between flight and momentum vectors be < 40 mrad.

We make several particle identification (PID) requirements to ensure the identity of the signal pions and kaons. Tracks in $\eta_{3\pi}$ candidates must have DIRC, dE/dx, and EMC responses consistent with pions. For the charged $B^+ \to \eta K^+$ decay, the prompt charged track must have an associated DIRC Cherenkov angle between $-5\,\sigma$ and $+2\,\sigma$ from the expected value for a kaon. For $B^+ \to \eta\pi^+$, the DIRC Cherenkov angle must be between $-2\,\sigma$ and $+5\,\sigma$ from the expected value for a pion.

A B meson candidate is characterized kinematically by the energy-substituted mass $m_{\rm ES} = \sqrt{(\frac{1}{2}s + \mathbf{p}_0 \cdot \mathbf{p}_B)^2/E_0^2 - \mathbf{p}_B^2}$ and energy difference $\Delta E = E_B^* - \frac{1}{2}\sqrt{s}$, where the subscripts 0 and B refer to the initial $\Upsilon(4S)$ and to the B candidate, respectively, and the asterisk denotes the $\Upsilon(4S)$ frame. The resolutions on these quantities measured for signal events are 30 MeV and 3.0 MeV/c^2, respectively. We require $|\Delta E| \leq 0.2$ GeV and $5.2 \leq m_{\rm ES} \leq 5.29$ GeV/c^2 (the lower limit is 5.22 GeV/c^2 for $\eta_{\gamma\gamma}\pi^+$).

3.1 Tau, QED, and continuum background

To discriminate against tau-pair and two-photon background, we require in $\eta_{3\pi}$ channels that the event contain at least five (four) charged tracks for neutral (charged) B pairs. In $\eta_{\gamma\gamma}$ analyses, we require three (two) tracks for neutral (charged) B pairs.

To reject continuum background, we make use of the angle θ_T between the thrust axis of the B candidate and that of the rest of the tracks and neutral clusters in the event, calculated in the center-of-mass frame. The distribution of $\cos\theta_T$ is sharply peaked near ±1 for combinations drawn from jet-like $q\bar{q}$ pairs and is nearly uniform for the isotropic B meson decays; we require $|\cos\theta_T| < 0.9$. A second B candidate satisfying the selection criteria is found in about 10–20% of the events. In this case the "best" combination is chosen as the one closest to the nominal η mass.

The remaining continuum background dominates the samples and is modeled from sideband data for the maximum likelihood fits described in Section 4.

3.2 $B\overline{B}$ background

We use Monte Carlo simulations of $B^0\overline{B}^0$ and B^+B^- pair production and decay to look for possible $B\overline{B}$ backgrounds. Most $B\overline{B}$ backgrounds in these analyses come from other charmless decays. From these studies we find no evidence for significant $B\overline{B}$ background in the $\eta \to \pi^+\pi^-\pi^0$ decay chains.

For the $\eta \to \gamma\gamma$ modes we find potential $B\overline{B}$ backgrounds from several charmless final states, which we treat with additional event selection criteria. To reduce background from $\pi^0\pi^+$, π^0K^+, and π^0K^0, we eliminate $\eta_{\gamma\gamma}$ candidates that share a photon with any π^0 candidate having momentum between 1.9 and 3.1 GeV/c in the $\Upsilon(4S)$ frame. Additionally, we remove high-energy photons to suppress background from $K^*\gamma$, by requiring $E_\gamma < 2.4$ GeV. We find a small remaining $B\overline{B}$ background in $\eta_{\gamma\gamma}\pi$ ($\eta_{\gamma\gamma}K$) from $\eta\rho$ (ηK^*). To discriminate between these and the signal we include a $B\overline{B}$ component in the likelihood fits for modes with $\eta \to \gamma\gamma$, as described in Section 4.1.

4 Maximum Likelihood Fit

We use an unbinned, multivariate maximum-likelihood fit to extract signal yields for our modes. A sample of events to fit is selected as described in Section 3.

4.1 Likelihood Function

The likelihood function incorporates four uncorrelated variables. We describe the B decay kinematics with two variables: ΔE and $m_{\rm ES}$. We also include m_η and a Fisher discriminant $\mathcal{F}$ which describes energy flow in the event. The Fisher discriminant combines four variables: the angles with respect to the beam axis, in the $\Upsilon(4S)$ frame, of the B momentum and B thrust axis, and the zeroth and second angular moments $L_{0,2}$ of the energy flow about the B thrust axis. The moments are defined by

$$L_j = \sum_i p_i \times |\cos\theta_i|^j \,, \tag{1}$$

where θ_i is the angle with respect to the B thrust axis of track or neutral cluster i, p_i is its momentum, and the sum excludes the B candidate.

As measured correlations among the observables in the selected data are small, we take the probability distribution function (PDF) for each event to be a product of the PDFs for the separate observables. We define hypotheses j, where j can be signal, continuum background, or (for modes with $\eta_{\gamma\gamma}$) $B\overline{B}$ background. The product PDF (to be evaluated with the observable set for event i) is then given by

$$\mathcal{P}_j^i = \mathcal{P}_j(m_{\rm ES}) \cdot \mathcal{P}_j(\Delta E) \cdot \mathcal{P}_j(\mathcal{F}) \cdot \mathcal{P}_j(m_\eta). \tag{2}$$

The likelihood function for each decay mode is

$$\mathcal{L} = \frac{\exp\left(-\sum_j Y_j\right)}{N!} \prod_i^N \sum_j Y_j \mathcal{P}_j^i \,, \tag{3}$$

where Y_j is the yield of events of hypothesis j found by the fitter, and N is the number of events in the sample. The first factor takes into account the Poisson fluctuations in the total number of events.

4.2 Signal and Background Parameterization

We determine the PDFs for signal and $B\overline{B}$ background from MC distributions in each observable. For the continuum background we establish the functional forms and initial parameter values of the PDFs with data from sidebands in $m_{\rm ES}$ or ΔE. We allow several background parameters to float in the final fit.

The distributions in m_η, and in $m_{\rm ES}$ and ΔE for signal, are parameterized as Gaussian functions, with a second or third Gaussian as required for good fits to these samples. Slowly varying distributions (combinatoric background under the η mass and ΔE peaks) are parameterized by linear functions. The combinatoric background in $m_{\rm ES}$ is described by a phase-space-motivated empirical function [17]. We model the $\mathcal{F}$ distribution using a Gaussian function with different widths above and below the mean, and include a linear contribution of 1–3% in area to account for outlying events. The linear term ensures that the significance of the signal is not overestimated relative to background. Because of the rarity of outlying events this component is not particularly well determined in some data samples, but we have checked that the yield and its significance are insensitive to choices of a linear component over the conservative range 1–6%.

We check the simulation on which we rely for signal PDFs by comparing with large data control samples. For $m_{\rm ES}$ and ΔE we use the decays $B^- \to \pi^- D^0$, $D^0 \to K^-\pi^+\pi^0$, which have similar topology to the modes under study. For m_η we use inclusive resonance production.

5 Fit Results

By generating (from PDF shapes) and fitting simulated samples of signal and background, we verify that our fitting procedure is functioning properly. We find that the minimum $\ln\mathcal{L}$ value in the on-resonance sample lies well within the $\ln\mathcal{L}$ distribution from these simulated samples.

The efficiency is obtained from the fraction of signal MC events passing the selection, adjusted for any bias in the likelihood fit. This bias is determined from fits to simulated samples, each equal in size to the data and containing a known number of signal MC events combined with events generated from the background PDFs. We find biases ranging from 1% to 4%, depending on the mode.

Table 2: Final fit results for $B^+ \to \eta h^+$ and $B^0 \to \eta K^0$, where $\eta \to \pi^+\pi^-\pi^0$ and $\eta \to \gamma\gamma$. We report branching fractions for the two η decay channels separately ($\mathcal{B}$) and after combining the results of the two channels (Combined $\mathcal{B}$). Systematic contributions are included in the signficance values. The Corrected $\mathcal{B}$ for the charged modes is the branching fraction after correcting for crossfeed from one charged mode into the other.

Fit quantity	$\eta_{3\pi}\pi^+$	$\eta_{\gamma\gamma}\pi^+$	$\eta_{3\pi}K^+$	$\eta_{\gamma\gamma}K^+$	$\eta_{3\pi}K^0$	$\eta_{\gamma\gamma}K^0$
Fit sample size						
On-resonance	9477	6933	5383	5884	1270	1435
Off-resonance	1104	1168	630	959	158	183
Signal yield						
On-res data	$28.0^{+10.0}_{-8.8}$	$39.6^{+11.3}_{-10.1}$	$14.4^{+8.2}_{-7.0}$	$34.3^{+9.8}_{-8.8}$	$2.6^{+4.1}_{-3.1}$	$8.6^{+4.8}_{-3.8}$
Off-res data	$1.1^{+2.1}_{-1.2}$	$0.0^{+2.3}_{-0.0}$	$0.6^{+3.9}_{-2.9}$	$0.0^{+0.7}_{-0.0}$	$0.0^{+0.7}_{-0.0}$	$0.0^{+0.8}_{-0.0}$
Selection ϵ (%)	23.3	28.7	22.6	30.6	22.6	24.8
$\prod\mathcal{B}_i$ (%)	22.6	39.4	22.6	39.4	7.8	13.5
$\epsilon\times\prod\mathcal{B}_i$ (%)	5.2	11.3	5.1	12.1	1.76	3.34
Stat. sign. (σ)	4.3	5.7	2.4	5.7	0.8	3.2
$\mathcal{B}(\times10^{-6})$	$6.0^{+2.1}_{-1.9}$	$3.9^{+1.1}_{-1.0}$	$3.2^{+1.8}_{-1.5}$	$3.2^{+0.9}_{-0.8}$	$1.7^{+2.6}_{-2.0}$	$2.9^{+1.6}_{-1.3}$
Combined $\mathcal{B}$	$4.5^{+1.0}_{-0.9}\pm0.3$		$3.2^{+0.8}_{-0.7}\pm0.2$		$2.6^{+0.9}_{-0.8}\pm0.2$	
Stat. sign. (σ)	7.0		6.2		3.3	
Corrected $\mathcal{B}$	$4.2^{+1.0}_{-0.9}\pm0.3$		$2.8^{+0.8}_{-0.7}\pm0.2$		$2.6^{+0.9}_{-0.8}\pm0.2$	
90% C.L. UL(incl. syst.)	—		—		<4.6	
Bkg $\mathcal{A}_{ch}$	-0.00 ± 0.01	-0.02 ± 0.01	-0.02 ± 0.01	-0.00 ± 0.01	–	–
Signal $\mathcal{A}_{ch}$	-0.50 ± 0.31	-0.51 ± 0.24	-0.56 ± 0.55	-0.25 ± 0.26	–	–
Combined $\mathcal{A}_{ch}$	$-0.51^{+0.20}_{-0.18}\pm0.01$		$-0.32^{+0.22}_{-0.18}\pm0.01$		–	
Stat. sign. (σ)	2.5		1.4			

In Table 2 we show the results of the fits for off- and on-resonance data. Shown for each decay mode are the number of events that were fit, the signal yield, the efficiency (ϵ) and daughter branching fraction product ($\prod\mathcal{B}_i$), and the central value of the branching fraction. We also show the

branching fraction results after combining the two η decay channels, before and after a correction for crossfeed between the two charged channels (see Section 7), and the statistical significance of this combined result. For ηK^0 we quote a 90% CL upper limit. The statistical error on the number of events is taken as the change in the central value when the quantity $-2\ln\mathcal{L}$ changes by one unit. The statistical significance is taken as the square root of the difference between the value of $-2\ln\mathcal{L}$ for zero signal and the value at its minimum. For the charged modes we also give the charge asymmetry $\mathcal{A}_{ch}$.

In Fig. 1 we show projections of $m_{\rm ES}$ and ΔE made by selecting events with signal likelihood (computed without the variable shown in the figure) exceeding a mode-dependent threshold that optimizes the expected sensitivity.

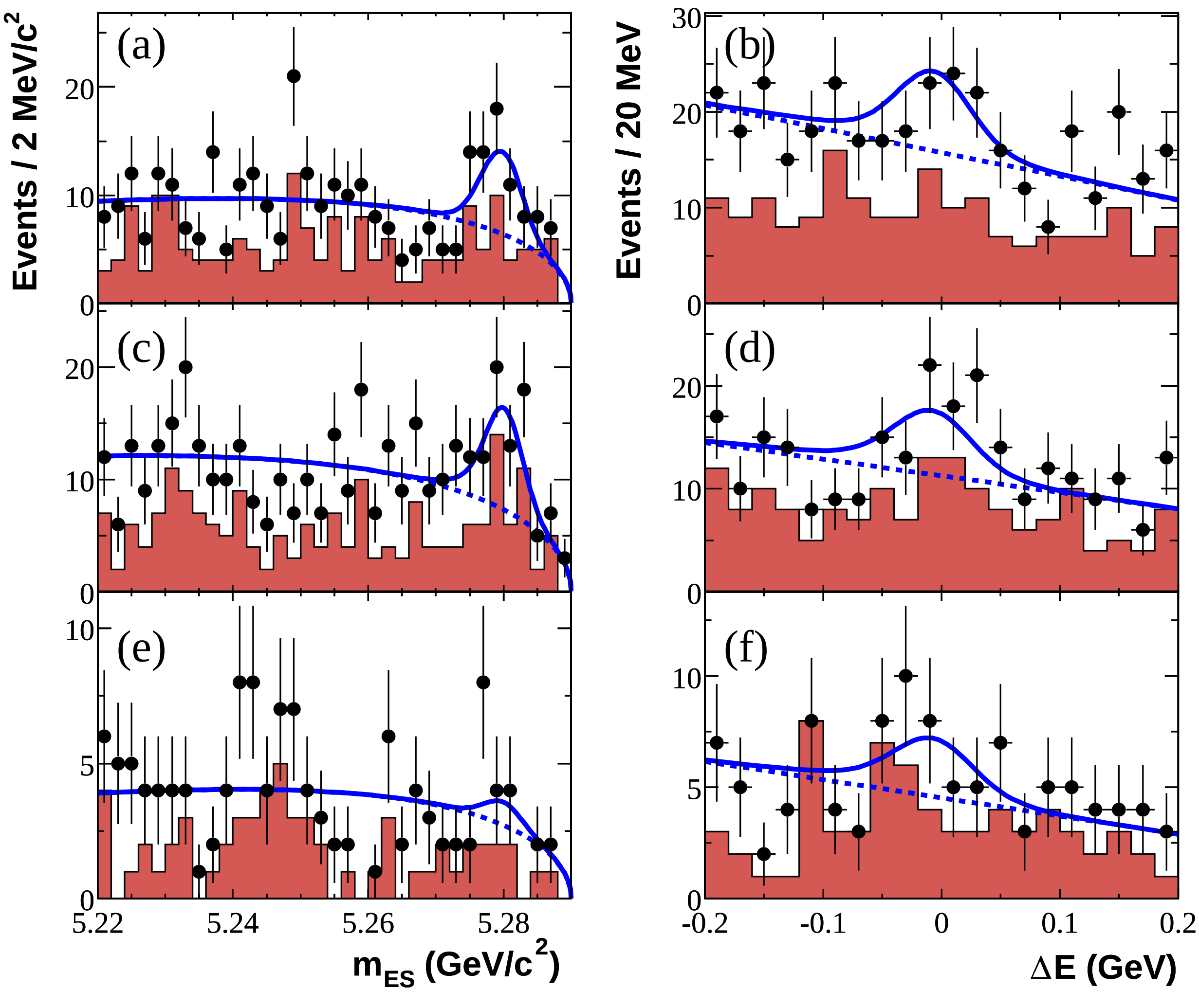

Figure 1: Projections of the B candidate $m_{\rm ES}$ and ΔE for $B^+ \to \eta\pi^+$ (a, b), $B^+ \to \eta K^+$ (c, d), and $B^0 \to \eta K^0$ (e, f). Points with errors represent data, shaded histograms the $\eta_{\gamma\gamma}$ subset, solid curves the full fit functions, and dashed curves the background functions. These plots are made with a cut on the signal likelihood and thus do not show all events in the data samples.

6 Systematic Uncertainties

Most of the systematic errors on yields that arise from uncertainties in the values of the PDF parameters have already been incorporated into the overall statistical error, because their background parameters are free in the fit. We determine the sensitivity to parameters of the signal PDF components by varying these within their uncertainties. The results are shown in the first row of Table 3. This is the only systematic error on the fit yield; the other systematics apply to either the efficiency or the number of $B\overline{B}$'s.

The uncertainty in our knowledge of the efficiency is found to be $0.8N_t\%$, $2.5N_\gamma\%$, and 3% for a K_S^0 decay, where N_t and N_γ are the number of signal tracks and photons, respectively. We estimate the uncertainty in the number of produced $B\overline{B}$ pairs to be 1.1%. The estimate of systematic bias from the fitter itself (1–2%) comes from fits of simulated samples with varying background populations. Published world averages [18] provide the B daughter branching fraction uncertainties. We account for systematic effects in $\cos\theta_{\rm T}$ (1%) and in the PID requirement (0.5%) on the prompt charged track. Values for each of these contributions are given in Table 3.

A study of the charge asymmetry as a function of momentum for all tracks in hadronic events bounds the tracking efficiency component of charge-asymmetry bias to be less than 1%. Samples of B and D^*-tagged $D \to K\pi$ decays provide additional crosschecks that the bias is small. We assign a systematic uncertainty for $\mathcal{A}_{ch}$ of 1.1% based on the tracking study and a small PID contribution determined from the D^* studies.

Table 3: Estimates of systematic errors (in percent) for the $B^+ \to \eta h^+$ and $B^0 \to \eta K^0$ modes. We specify which systematics are uncorrelated (U) or correlated (C) between η decay channels.

Quantity	$\eta_{3\pi}\pi^+$	$\eta_{\gamma\gamma}\pi^+$	$\eta_{3\pi}K^+$	$\eta_{\gamma\gamma}K^+$	$\eta_{3\pi}K^0$	$\eta_{\gamma\gamma}K^0$
Fit yield (U)	3.9	3.7	8.4	4.5	20.7	2.3
Fit efficiency/bias (U)	1.9	1.3	1.3	0.8	1.0	1.7
Track multiplicity (C)	1.0	1.0	1.0	1.0	1.0	1.0
Tracking eff/qual (C)	2.4	0.8	2.4	0.8	3.7	2.1
$\pi^0/\eta/\gamma$ eff (C)	5.0	5.0	5.0	5.0	5.0	5.0
K_S^0 efficiency (C)	—	—	—	—	2.9	2.9
Number $B\overline{B}$ (C)	1.1	1.1	1.1	1.1	1.1	1.1
Branching fractions (U)	1.0	1.0	1.0	1.0	1.0	1.0
MC statistics (U)	1.1	1.1	1.0	1.1	1.1	1.0
$\cos\theta_{\rm T}$(C)	1.0	1.0	1.0	1.0	1.0	1.0
PID (C)	1.4	1.0	1.4	1.0	1.0	—
Total	7.5	6.9	10.5	7.3	22.0	7.2
Uncorrelated	4.6	4.2	8.6	4.8	20.8	3.2
Correlated	6.0	5.5	6.0	5.5	7.2	6.4

7 Combined Results

We next combine the $\eta \to 3\pi$ and $\eta \to \gamma\gamma$ branching fraction measurements. We do this by first forming for each η decay mode the convolution of $\mathcal{L}$ from the fit with a Gaussian function representing the uncorrelated systematic error. The curves $-2\ln\mathcal{L}$ are shown in Fig. 2, for each η mode and for their sum. For the time integrated charge asymmetries the corresponding $-2\ln\mathcal{L}$ plots are given in Fig. 3.

The results at this stage are given in the row labeled "Combined $\mathcal{B}$" in Table 2. For the charged modes we must apply a correction for kaon–pion crossfeed arising from imperfect PID. In studies with kaon and pion samples tagged kinematically from the decays $D^{*+} \to \pi^+ D^0$, $D^0 \to K^-\pi^+$ we find that $9\pm2\%$ of pions are accepted by our kaon selection and vice versa. After correcting for this and adding the associated systematic uncertainty we obtain the final measurements summarized in Section 8.

8 Conclusion

We report preliminary measurements of branching fractions and $\mathcal{A}_{ch}$ for B meson decays to η with a charged kaon or pion, as well as the branching fraction for $B^0 \to \eta K^0$. We find statistically significant signals in the charged B decays. The branching fractions are

$$\begin{aligned} \mathcal{B}(B^+ \to \eta\pi^+) &= (4.2^{+1.0}_{-0.9} \pm 0.3) \times 10^{-6}\,, \\ \mathcal{B}(B^+ \to \eta K^+) &= (2.8^{+0.8}_{-0.7} \pm 0.2) \times 10^{-6}. \end{aligned}$$

For the neutral B decay, we find $\mathcal{B}(B^0 \to \eta K^0) = (2.6^{+0.9}_{-0.8} \pm 0.2) \times 10^{-6}$. Since the statistical significance of this result is only 3.3σ, we determine a 90% CL upper limit:

$$\mathcal{B}(B^0 \to \eta K^0) \;<\; 4.6 \times 10^{-6}.$$

These results supersede the previous *BABAR* measurements [12]. Our measurements of the *CP*-violating charge asymmetries in the charged modes are

$$\begin{aligned} \mathcal{A}_{ch}(B^+ \to \eta\pi^+) &= -0.51^{+0.20}_{-0.18} \pm 0.01\,, \\ \mathcal{A}_{ch}(B^+ \to \eta K^+) &= -0.32^{+0.22}_{-0.18} \pm 0.01. \end{aligned}$$

These charge asymmetry results are in agreement with the theoretical expectations discussed in Section 1 and rule out substantial positive asymmetries.

9 Acknowledgments

We are grateful for the extraordinary contributions of our PEP-II colleagues in achieving the excellent luminosity and machine conditions that have made this work possible. The success of this project also relies critically on the expertise and dedication of the computing organizations that support *BABAR*. The collaborating institutions wish to thank SLAC for its support and the kind hospitality extended to them. This work is supported by the US Department of Energy and National Science Foundation, the Natural Sciences and Engineering Research Council (Canada), Institute of High Energy Physics (China), the Commissariat à l'Energie Atomique and Institut National de Physique Nucléaire et de Physique des Particules (France), the Bundesministerium für

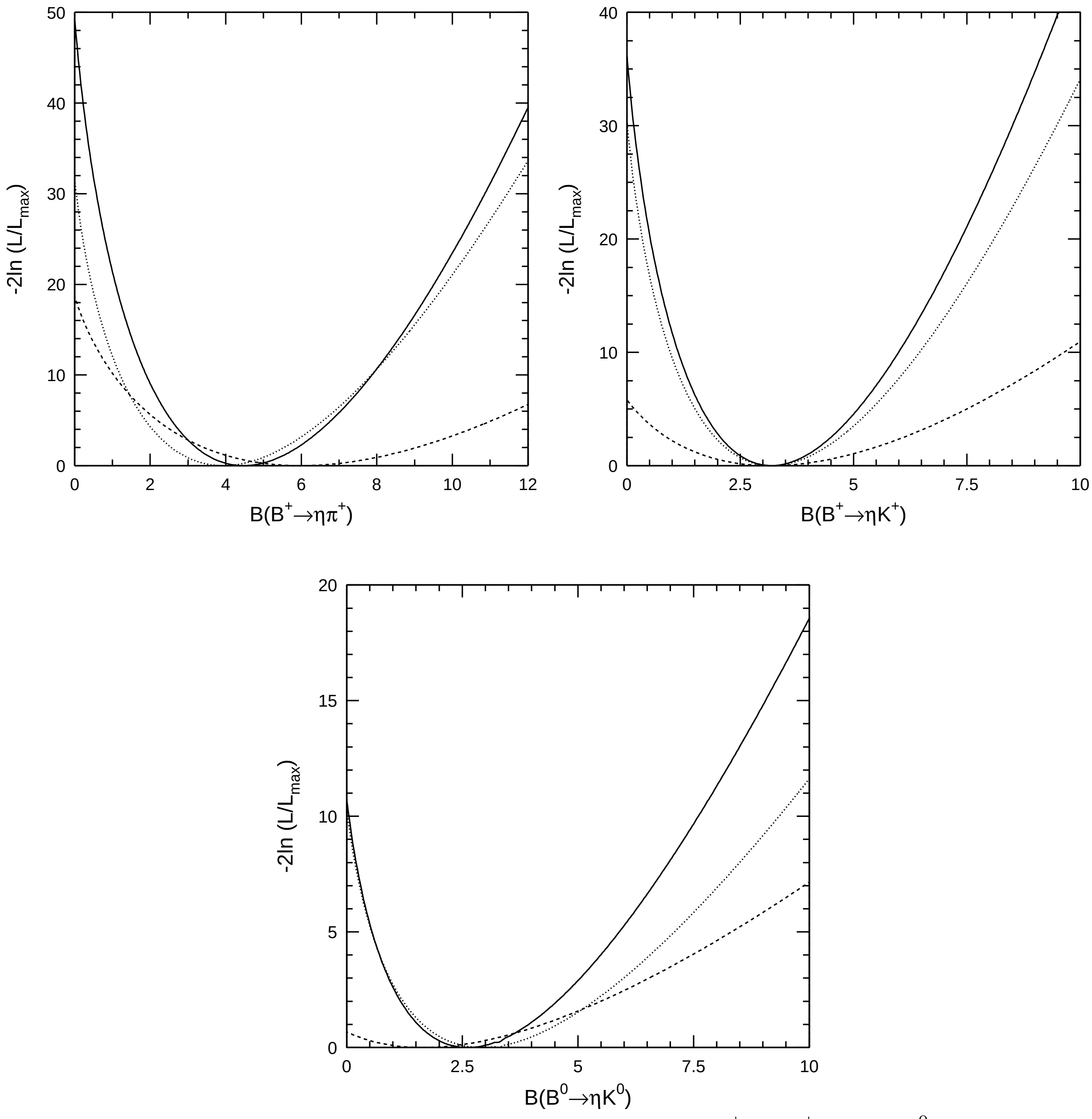

Figure 2: Distributions of $-2\ln\mathcal{L}$ vs branching fraction for $\eta\pi^+$, ηK^+ and ηK^0 decays. Two secondary channels (dashed and dotted lines) are combined to produce a final result (solid line). The dashed line corresponds to $\eta \to \pi^+\pi^-\pi^0$ decays, while the dotted line corresponds to $\eta \to \gamma\gamma$.

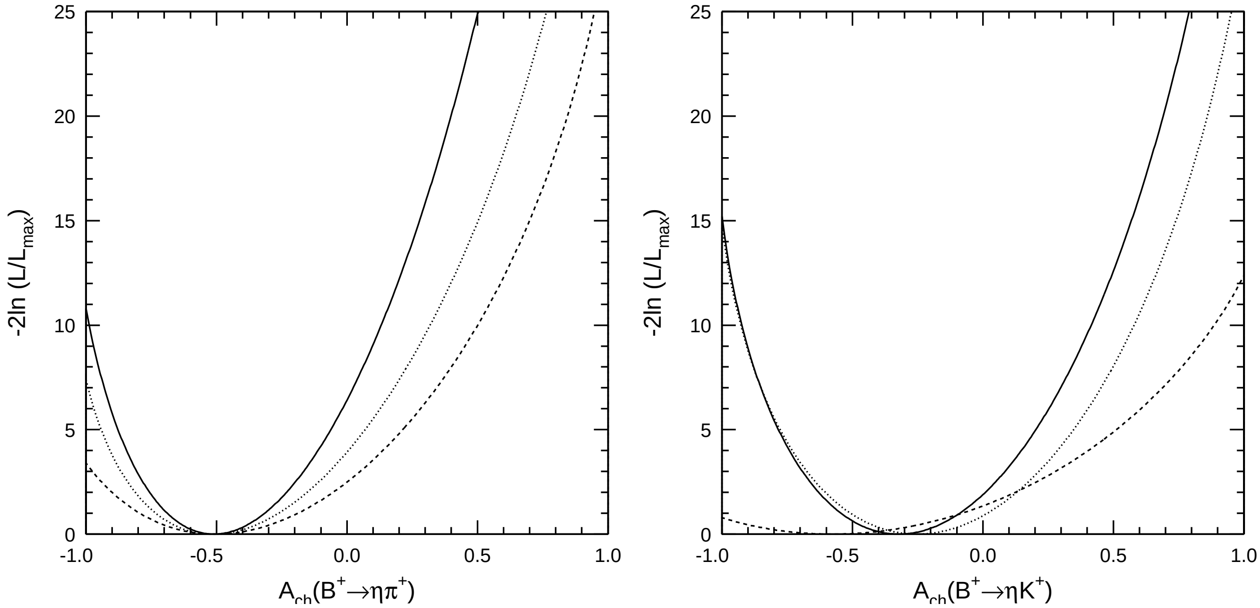

Figure 3: Distributions of $-2\ln\mathcal{L}$ vs $\mathcal{A}_{ch}$ for $\eta\pi^+$and ηK^+ decays. Two secondary channels (dashed and dotted lines) are combined to produce a final result (solid line). Dashed line corresponds to $\eta \to \pi^+\pi^-\pi^0$ decays, while the dotted line corresponds to $\eta \to \gamma\gamma$.

Bildung und Forschung and Deutsche Forschungsgemeinschaft (Germany), the Istituto Nazionale di Fisica Nucleare (Italy), the Foundation for Fundamental Research on Matter (The Netherlands), the Research Council of Norway, the Ministry of Science and Technology of the Russian Federation, and the Particle Physics and Astronomy Research Council (United Kingdom). Individuals have received support from the A. P. Sloan Foundation, the Research Corporation, and the Alexander von Humboldt Foundation.

References

[1] CLEO Collaboration, B. H. Behrens *et al.*, Phys. Rev. Lett. **80**, 3710 (1998).

[2] H. J. Lipkin, Phys. Lett. B **254**, 247 (1991).

[3] M. Bander, D. Silverman, and A. Soni, Phys. Rev. Lett. **43**, 242 (1979).

[4] S. Barshay, D. Rein, and L.M. Sehgal, Phys. Lett. B **259**, 475 (1991).

[5] A.S. Dighe, M. Gronau, and J.L. Rosner, Phys. Rev. Lett. **79**, 4333 (1997).

[6] G. Kramer, W.F. Palmer, and H. Simma, Nucl. Phys. B **428**, 77 (1994).

[7] A. Ali, G. Kramer, and C.-D. Lü, Phys. Rev. D **59**, 014005 (1999). These authors use the opposite sign convention for $\mathcal{A}_{ch}$ than the one used in this paper.

[8] M.-Z. Yang and Y.-D. Yang, Nucl. Phys. B **609**, 469 (2001).

[9] M. Beneke and M. Neubert, Nucl. Phys. B **651**, 225 (2003).

[10] C.-W. Chiang and J. L. Rosner, Phys. Rev. D **65**, 074035 (2002).

[11] CLEO Collaboration, S. J. Richichi *et al.*, Phys. Rev. Lett. **85**, 520 (2000).

[12] P. Bloom, Proceedings of the 2002 SLAC Summer Institute, hep-ex/0302030 (2003).

[13] H.C. Huang (for the Belle Collaboration), hep-ex/0205062, Moriond 2002 contributed paper (2002).

[14] *BABAR* Collaboration, B. Aubert *et al.*, Nucl. Instr. Meth. A **479**, 1 (2002).

[15] PEP-II Conceptual Design Report, SLAC-R-418 (1993).

[16] The *BABAR* detector Monte Carlo simulation is based on GEANT: S. Agostinelli *et al.*, CERN-IT-20020003, KEK Preprint 2002-85, SLAC-PUB-9350, submitted to Nucl. Instr. Meth. A .

[17] With $x \equiv m_{\rm ES}/E_b$ and ξ a parameter to be fit, $f(x) \propto x\sqrt{1-x^2}\exp\left[-\xi(1-x^2)\right]$. See ARGUS Collaboration, H. Albrecht *et al.*, Phys. Lett. B **241**, 278 (1990).

[18] Particle Data Group, K. Hagiwara *et al.*, Phys. Rev. D **66**, 010001 (2002).